stellarator news

Published by Fusion Energy Division, Oak Ridge National Laboratory
Building 9201-2 P.O. Box 2009 Oak Ridge, TN 37831-8071, USA

Editor: James A. Rome Issue 60 November 1998
E-Mail: jar@ornl.gov Phone (423) 574-1306 Fax: (423) 576-3647
On the Web at *http://www.ornl.gov/fed/stelnews*

Pseudosymmetry, "water," and NCSX

It has long been realized that large neoclassical losses of particles and energy represent the most serious disadvantage of stellarators. The three-dimensional (3D) geometry of the magnetic fields in a stellarator typically leads to large variations in field strength along magnetic field lines. In general, this causes charged particles to have large excursions from the magnetic surface, leading to unacceptably large transport coefficients.

In the last 20 years, many efforts have been made to improve stellarator magnetic configurations. One of the most promising ideas advanced during this period is that of quasisymmetry (QS) [1]. Certain choices of the plasma column boundary shape can make 3D configurations appear to be 2D configurations from the viewpoint of the charged particle drift motion.

In such quasi-2D configurations, an additional invariant of the drift motion is conserved, so the transport losses in stellarators become of the same order as those in tokamaks.

Several analytical calculations, such as the paraxial approximation, and 3D numerical calculations have been performed to search for quasisymmetric stellarator configurations. It is generally difficult to satisfy QS and stability (e.g., ballooning) simultaneously. Thus some efforts have been made to generalize and to simplify the QS conditions.

The new concept of pseudosymmetry enlarges the parameter space of stellarators with good confinement. The definition of pseudosymmetry is the absence of locally trapped particles or equivalently, of ripples of mod B along the force line. The condition of pseudosymmetry is generally not as strong as QS.

By minimizing the amount of "water" contained in the ripples of mod B, we have obtained a pseudosymmetric configuration for consideration in the National Compact Stellarator Experiment (NCSX) being designed at Prince-

In this issue . . .

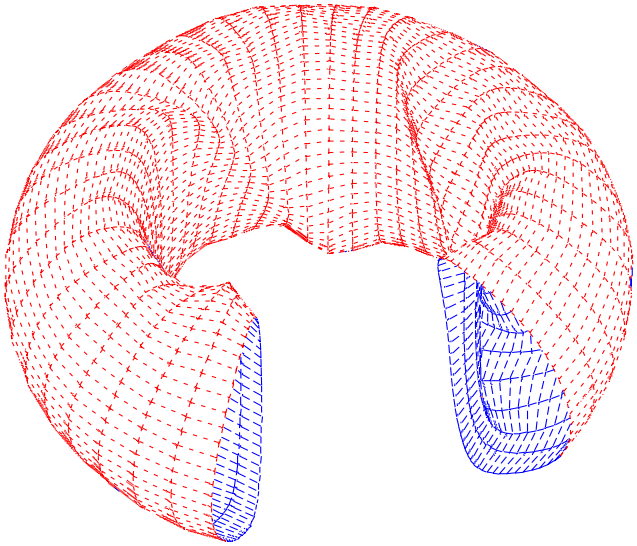

Fig. 1. *ksa14_11*, a 4-period quasiaxisymmetric configuration candidate for NCSX.

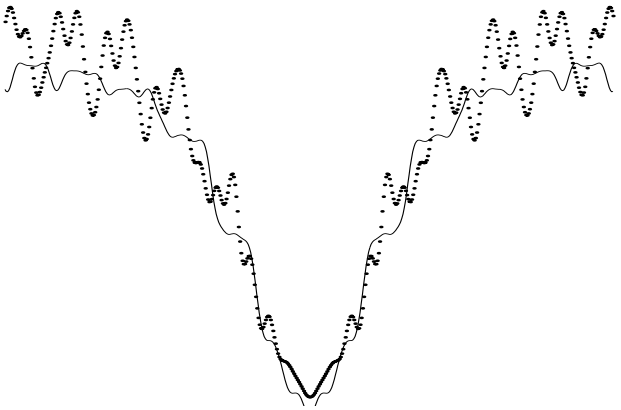

Fig. 2. Mod *B* along a field line before (dotted line) and after (solid line) optimization.

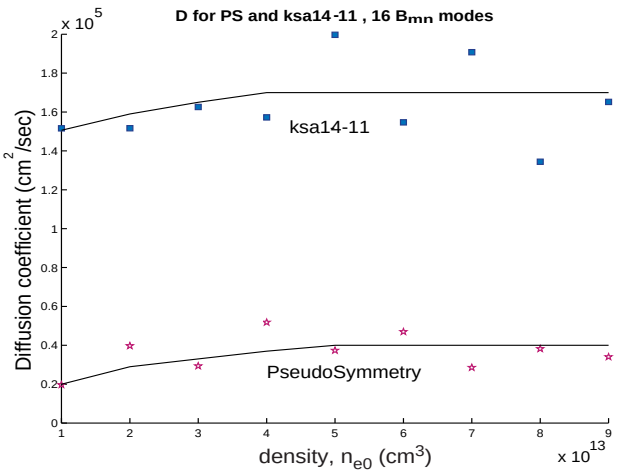

Fig. 3. Diffusion coefficient before and after optimization.

ton Plasma Physics Laboratory. The configuration used as a starting point for our pseudosymmetrization is, *ksa14_11*, a 4-period quasiaxisymmetric configuration (Fig. 1). *ksa14_11* uses helical stellarator fields to obtain a ballooning stable configuration. These helical fields produce large mod *B* ripples along the force line and correspondingly significant transport losses.

To improve the ripple transport properties of *ksa14_11* we used the "water" target function as a tool to obtain a pseudosymmetric configuration. As a result of this optimization the amount of "water" was reduced by a factor of 10 (see Fig. 2). To verify the good transport properties we calculated of the diffusion coefficient *D* using the GC3 code of H. Mynick [2]. These calculations demonstrate a 5-fold decrease of the value of *D* for the optimized configuration (Fig. 3).

In conclusion, we have shown that the "water" target function can be used effectively to achieve pseudosymmetry and to vastly improve transport properties in stellarator configurations.

References

[1] J. Nührenburg and R. Zille, Phys. Lett. A **129** (1988) 113.

[2] H. E. Mynick, Plasma Physics Rep. **23** (1997) 547.

M. Isaev, M. Mikhailov, A. Subbotin
RRC Kurchatov Institute, Moscow, Russia
D. Monticello, H. Mynick
Princeton Plasma Physics Laboratory, Princeton, U.S.A.

Confinement, fluctuations, and electric fields in the H-1 heliac

Introduction

The H-1 heliac [1] is a medium-sized helical axis stellarator experiment with a major radius R = 1 m, and an average plasma minor radius a = 0.15–0.2 m. Its "flexible heliac" [2] coil set permits both extraordinary variation in the low-shear rotational transform profile in the range 0.6 < ι < 2.0 and variable average magnetic well. The ultimate design ratings of the H-1 facility are toroidal magnetic field B = 1 T and heating power P ~500 kW. However, during its initial operating period, experiments have been limited to lower magnetic field, B = 0.2 T, and P = 100 kW, and we have concentrated on studying confinement phenomena in low-density discharges. These discharges are produced in helium, neon, and argon using 50–100 kW of high-cyclotron harmonic helicon wave heating (f = 7 MHz) and typically have pulse lengths of 80 ms, electron densities $n_e = (0.5–2) \times 10^{12}$ cm^{-3}, electron temperatures T_e = 10–30 eV, and ion energies T_i = 50–100 eV. These plasmas are diagnosed by a variety of probe and optical techniques. A particular advantage of operation at low magnetic field and temperature is that the interpretation of Langmuir probe data is simplified.

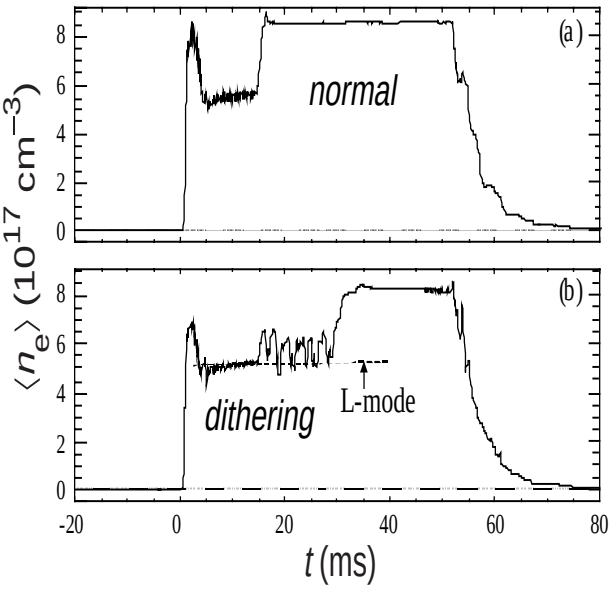

Fig. 1. Time traces of the line-average density in H-1 discharges, showing (a) normal and (b) "dithering" transitions to high confinement.

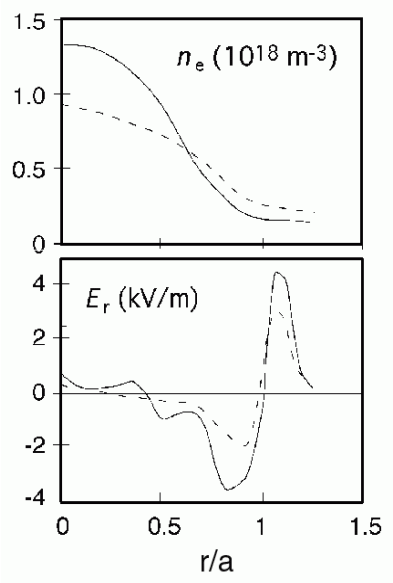

Fig. 2. Radial profiles of plasma density n_e and radial electric field E_r in H-1. Profiles taken 5 ms before (dotted) and 5 ms after (solid) transition to improved confinement. The plasma boundary r/a = 1 is determined by the last closed magnetic flux surface and is also the location of the helicon wave antenna.

Confinement transitions and the electric field

For magnetic fields above a critical value that depends on pressure and somewhat on magnetic configuration, the plasma undergoes a transition (Fig. 1) during which the line-average density doubles, the density gradient increases (Fig. 2), and the average ion energy increases markedly. These transitions can occur singly or as a sequence of forward/backward "dithering" jumps. They are accompanied by a deepening of the potential well, an increase in the magnitude of the inwardly pointing radial electric field, a reduction in turbulence levels, and a reduction or even reversal in the (normally outward) fluctuation-induced particle flux (as measured using Langmuir probe techniques) [3, 4]. These phenomena are remarkably similar to those seen during L-H transitions in larger tokamaks and stellarators with heating in the megawatt range [5], making H-1 a useful model experiment.

As with any confined plasma, the radial electric field is determined by the constraint of quasineutrality and the balance of the outward ion and electron fluxes. In the low-magnetic-field regime in which H-1 is now operated, the ion gyroradii are quite large, $\rho_i / a \sim 0.1–0.5$ (depending on the working gas), and computational studies of ion orbits show that direct losses remain important even when radial electric fields like those measured in the experiment are included. Modeling studies suggest that this radial electric field is nonetheless roughly consistent with ambipolar ion

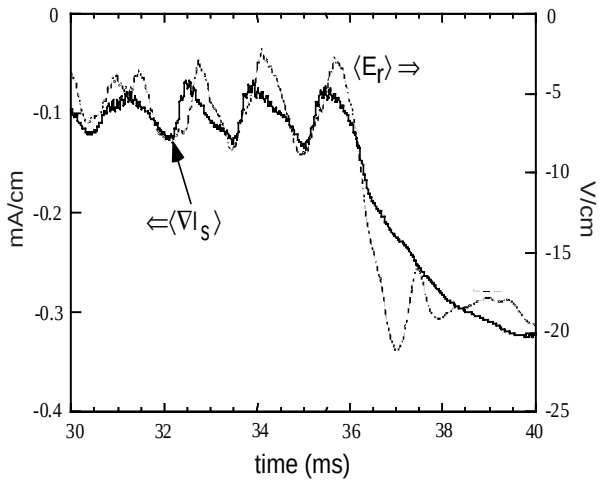

Fig. 3. Time traces of electric field and gradient of ion saturation current (measured with a Langmuir probe array) for a discharge with dithering transitions. The quantities are averaged over the radial region 0.25 < *r*/*a* < 1.

and electron fluxes when both diffusive and direct losses are included [4].

The transition to the high confinement mode exhibits a threshold dependence on magnetic field, pressure, and power. Analysis [4] of data from experiments in which the power was stepped up and down suggests that this behavior is compatible with a model in which the radial electric field is driven to a critical value depending upon the relative heating of the ions and electrons. Moreover, the jump to a higher electric field coincides with an increase in the ion pressure gradient. This is consistent with expectations for a radial force balance applied in H-1 discharges.

The interplay between radial electric field and pressure gradient was illustrated graphically in an experiment that took advantage of the dithering behavior shown in Fig. 1. A radial array of 24 Langmuir probes was used to measure the ion saturation current, electron temperature, floating potential, and plasma potential. Results from a sample dithering discharge are shown in Fig. 3. The time traces show the spatially averaged radial electric field and the gradient of the ion saturation current—which we take as a proxy for the ion pressure, since

$$I_{si} \propto n_i \, (T_e + T_i)^{1/2}$$

and $T_e < T_i$ in these discharges. As the discharge changes back and forth between low and high modes, the average electric field and "pressure" gradient oscillate with only a small phase lag.

Probe studies are also being used to determine the possible role of the radial structure of the radial electric field in the transition to high confinement. Figure 4 shows data from an experiment in which the Langmuir probe array was

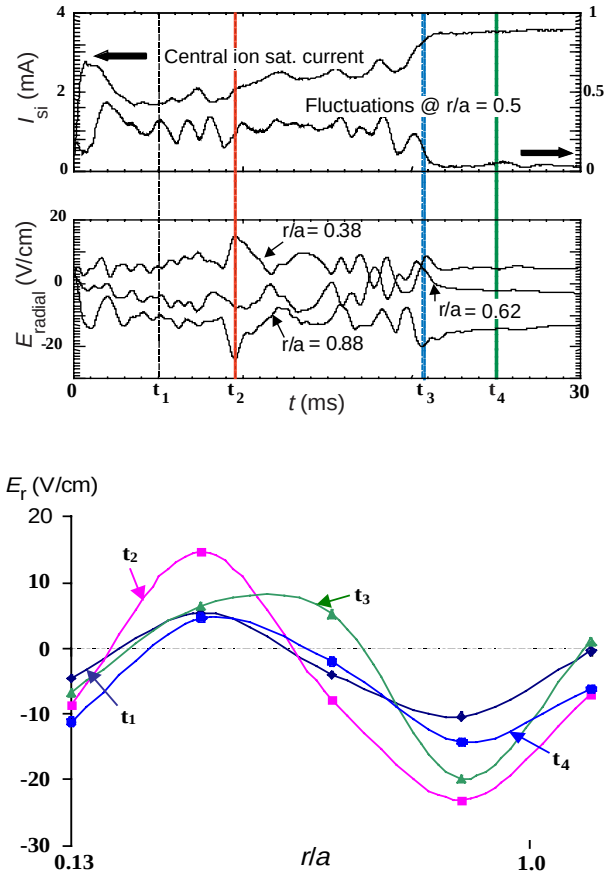

Fig. 4. Top: Time traces of signals from Langmuir probe array during a discharge with a confinement transition at t_3. Bottom: radial profiles of the radial electric field at the four times indicated in the time traces.

used to measure plasma parameters at six radial locations during a confinement transition. Profiles of the electric field were taken at the four times shown in the figure. For this particular discharge, the radial electric field in the region of strong pressure gradient at *r*/*a* ~ 0.5 increases as the fluctuations die out during the transition to high confinement. We emphasize that this effect is not seen in every discharge, so further experiments and extensive analysis will be required before drawing a conclusion that changes in gradients of the radial electric field coincide with the confinement transition.

Preparations are under way to increase the magnetic field to 0.5–1.0 T, to increase the low-frequency heating power to 250 kW, and to add 200 kW of 28-GHz ECH power. These improved capabilities will permit the decoupling of electron and ion heating and experiments at higher plasma densities and temperatures.

This work was supported by the Australian Department of Industry, Science, and Tourism and the Australian Institute of Nuclear Science and Engineering as part of the Major

National Research Facilities program.

REFERENCES

[1] S. M. HAMBERGER *et al*, Fusion Technol. **17** (1990) 123.

[2] J. H. HARRIS *et al.*, Nucl. Fusion **25** (1985) 623.

[3] M. G. SHATS *et al.*, Phys. Rev. Lett. **77** (1996) 4190.

[4] M. G. SHATS *et al.*, Physics of Plasmas **6** (1998) 2390

[5] F. WAGNER *et al.*, Phys. Rev. Lett. **49** (1982) 1408.

J. H. Harris, M. G. Shats, B. D. Blackwell, G. G. Borg, R. W. Boswell, A. D. Cheetham,[1] S. A. Dettrick, R. L. Dewar, H. J. Gardner, J. Howard, C. A. Michael, D. Miljak,[2] D. L. Rudakov

Plasma Research Laboratory
Australian National University
Canberra, ACT 0200 Australia

[1] University of Canberra
ACT 2601 Australia

[2] University of Sydney
NSW 2006 Australia

Initial experiments in the TJ-II Flexible Heliac

Two mobile poloidal limiters have been installed in TJ-II so that the interaction between the plasma and the vessel can be reduced when required. The influence of poloidal limiters on the scrape-off layer (SOL) thickness and on impurity fuelling, as compared with the limiting effect of other parts of the TJ-II vessel (helical limiter), has been studied. In the experiments reported here, the plasma has been exposed only to metallic (stainless steel) components.

Characteristics of the magnetic field and influence of plasma volume on confinement

Plasma configurations with a wide range of plasma volumes, 0.3–1.2 m^3, and average plasma radius in the range 0.12–0.22 m were chosen. The vacuum rotational transform profile is very flat [$\iota(0) \approx \iota(a) \sim 0.1$] and the magnetic well in the studied configurations is in the range 2–4%. Quasistationary discharges with electron cyclotron heating lasting up to 250 ms were obtained. The average electron density achieved was $\langle n_e \rangle \sim (0.5–1.0) \times 10^{19}$ m^{-3}, the central electron and ion temperatures, T_e and T_i, were ~0.4–0.8 keV and ~0.1 keV, respectively, and the stored energy W was ~0.8 kJ.

Electron temperature profiles obtained from second harmonic electron cyclotron emission (ECE) and multiposition Thomson scattering system measurements are shown in Fig. 1 for a series of discharges with $\iota(0) \sim 1.51$. Good agreement is found between the ECE, multiposition Thomson scattering, and Si(Li) detector measurements (when available). The central temperatures are about 600 eV for these discharges. The distortion of the profiles on the low-field side of the plasma is interpreted as being caused by a significant population of suprathermal electrons, which gives rise to ECE at downshifted frequencies. For these plasma conditions, the density profile is rather flat, whereas the temperature profile is peaked.

A rough estimation of the global particle confinement time can be obtained from $Vn_e/S\,\Gamma_{LCFS}$, where S is the plasma surface, V the volume, and Γ_{LCFS} the radial flux at the last closed flux surface. This ratio, which is in the range 5–8 ms, is consistent with H_α measurements if allowance for a moderate recycling coefficient is made.

Rotational transform scan and plasma profiles

The influence of natural plasma resonances on plasma profiles and confinement is being investigated. A magnetic configuration scan has been done to move the 8/5 resonance from the edge to the central region of the plasma. The natural 8/5 rational surface in the plasma boundary region, as predicted by equilibrium codes for this configu-

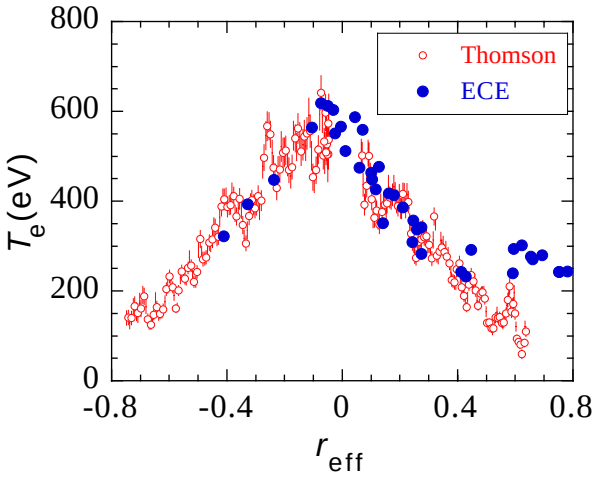

Fig. 1. Comparison of electron temperature profiles obtained from second harmonic ECE and Thomson scattering measurements; Thomson data are obtained in a single shot of the discharge series with ι(0) ~ 1.51. The maximum that appears on the low field side of the ECE profile is due to the presence of a suprathermal electron population.

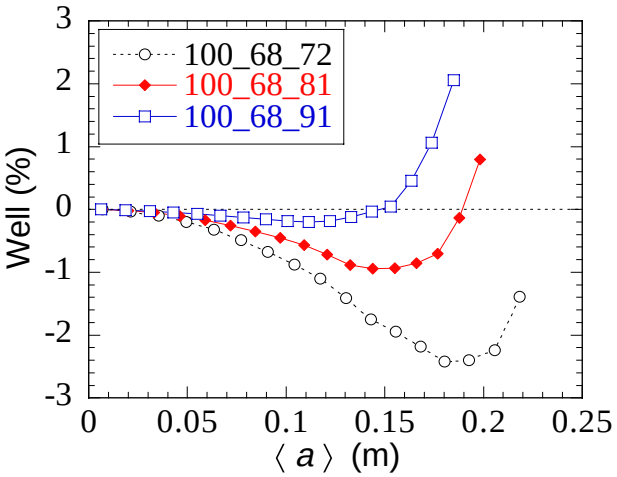

Fig. 2. Magnetic well radial profiles for the magnetic configurations investigated in the magnetic well scan experiment.

ration, has been observed as a flattening in the edge profiles (i.e., ion saturation current and floating potential). The 8/5 resonance does not appear to have a significant influence on global confinement properties. Further experiments are in progress to investigate the influence of major resonances on plasma profiles and confinement.

Magnetic well scan and plasma operation

The flexibility of TJ-II allows the magnetic well depth to be modified over a broad range of values (~ 0–6%). This high degree of flexibility makes the TJ-II device attractive for investigating transport characteristics close to pressure gradient instability thresholds. Magnetic configurations with fixed rotational transform [ι(0) ~ 1.8] but with the magnetic well varied from 0.2 to 2% are being studied. Figure 2 shows the magnetic well radial profile, $[V'(r) - V'(0)]/V'(0)$ for these configurations. The configuration with the smallest magnetic well (~ 0.2%) has magnetic hill in the outer plasma region ($r/a > 0.7$). Radial electric fields near the plasma boundary are of the order of 20 V/cm in the plasma configurations with a magnetic well of 2%. In the configuration with the smallest well (~0.2), this becomes ~2 V/cm. Work is under way to study the structure of pressure profiles and fluctuations in configurations with a wide range of magnetic well values.

Influence of poloidal limiter on edge plasma studies

The role of the mobile (poloidal) limiters on plasma profiles and their influence on impurity dilution effects have been studied in the plasma configuration with plasma volume of 1.2 m^3.

Radial profiles of ion saturation current and floating potential have been measured for different radial locations of the poloidal limiter. The shear layer moves inward as the poloidal limiter is inserted into the plasma edge region and the ion saturation scale length increases. The *e*-folding length for the ion saturation current increases from 1 cm when the poloidal limiter is removed from the plasma to 3 cm when the limiting effect of the poloidal limiter is dominant. This result is in good agreement with field mapping estimates for the characteristic connection length L_c (i.e., $\lambda \sim L_c^{1/2}$).

A systematic reduction in plasma fueling by wall impurities is observed as the poloidal limiter is inserted into the plasma, thus permitting better density control by external gas injection and localized recycling on the mobile limiters.

TJ-II Team
Asociación Euratom-CIEMAT para Fusión
Av. Complutense nº22
28040 Madrid, Spain

Selected stellarator abstracts from the IAEA Meeting

OV1/4: An overview of the Large Helical Device project

A. Iiyoshi et al.

The Large Helical Device (LHD) has successfully started running plasma confinement experiments after a long construction period of eight years. During the construction and machine commissioning phases, a variety of milestones have been attained in fusion engineering, which successfully led to the first operation, and the first plasma was ignited on March 31, 1998. Two experimental campaigns are planned in 1998. In the first campaign, the magnetic flux mapping clearly demonstrated a nested structure of magnetic surfaces. The first plasma experiments were conducted with second harmonic 84-GHz and 82.6-GHz ECH at a heating power input of 0.35 MW. The magnetic field was set at 1.5 T in the first year so as to accumulate experience using the superconducting coils. In the second campaign, auxiliary heating with NBI at 3 MW has been carried out. The averaged electron densities up to 6×10^{19} m^{-3}, central temperatures ranging 1.4 to 1.5 keV and stored energies up to 220 kJ have been attained despite the fact that impurity level is not yet minimized. The obtained scaling of energy confinement time has been found to be consistent with the ISS95 scaling law with some enhancement.

OV4/5: Confinement physics study in a small low-aspect-ratio helical device, CHS

S. Okamura et al.

The configuration parameter of the plasma position relative to the center of the helical coil winding is very effective metric for controlling the MHD stability and the trapped particle confinement in heliotron/torsatron systems. But these two characteristics are contradictory to each other in this parameter. The inward shifted configuration is favorable for the drift-orbit optimization but it is predicted unstable against the Mercier criterion. Various physics problems, such as electric field structure, plasma rotation and MHD phenomena, have been studied in CHS with a compromising intermediate position. With this standard configuration, CHS has supplied experimental results for understanding general toroidal confinement physics and low-aspect-ratio helical systems. In the recent experiments, it was found that a wide range of inward shifted configurations gives stable plasma discharges without any restriction to a special pressure profile. Such enhanced range of operation made it possible to study experimentally drift-orbit optimized configurations in heliotron/torsatron systems. The effect of configuration improvement was studied with plasmas in a low collisionality regime.

EX2/2: Transition from L mode to high ion temperature mode in CHS heliotron/torsatron plasmas

K. Ida et al.

A high ion temperature mode (high T_i mode) is observed for neutral beam heated plasmas in the Compact Helical System (CHS) heliotron/torsatron. The high T_i mode plasma is characterized by a high central ion temperature, $T_i(0)$, and is associated with a peaked electron density profile produced by neutral beam fueling with low wall recycling. Transition from L mode to high T_i mode has been studied in CHS. The central ion temperature in the high T_i mode discharges reaches to 1 keV which is 2.5 times higher than that in the L mode discharges. The ion thermal diffusivity is significantly reduced by a factor of more than 2–3 in the high T_i mode plasma. The ion loss cone is observed in neutral particle flux in the energy range of 1–6 keV with a narrow range of pitch angle ($90 \pm 10°$) in the high T_i mode. However, the degradation of ion energy confinement due to this loss cone is negligible.

EX2/3: Plasma confinement studies in LHD

M. Fujiwara et al.

The initial experiments of the Large Helical Device (LHD) have extended confinement studies on currentless plasmas to a large scale (R = 3.9 m, a = 0.6 m). Heating by NBI of 3 MW has produced plasmas with a fusion triple product of 8×10^{18} keV·m^{-3}s at a magnetic field of 1.5 T. An electron temperature of 1.5 keV and an ion temperature of 1.1 keV have been achieved simultaneously at the line-averaged electron density of 1.5×10^{19} m^{-3}. The maximum stored energy has reached 0.22 MJ with neither unexpected confinement deterioration nor visible MHD instabilities, which corresponds to $\langle\beta\rangle$ =0.7%. Energy confinement times, reaching 0.17 s at the maximum, have shown a manner similar to the present scaling law derived from the existing medium sized helical devices, but improve on it by 50%. A distinguishing feature of a favorable dependence of energy confinement time on density remains in the present power density (~40 kW/m^3) and the electron density (3×10^{19}m^{-3}) regimes unlike L-mode in tokamaks. Temperatures of both electrons and ions as high as 200 eV have been observed at the outermost flux surface, which indicates a qualitative jump in performance from the helical devices to date. Spontaneously generated toroidal currents agree with the physical picture of neoclassical bootstrap currents. Change of magnetic configuration due to finite-beta effect has been well described by the 3-D MHD equilibrium analysis. An escape of particles from the core region leading to a hollow density profile has been observed in hydrogen plasmas, which is mitigated through core fueling with a pellet injection or in helium discharges.

EX5/1: Dynamic behavior associated with electric field transitions in CHS heliotron/torsatron

A. Fujisawa et al.

A new kind of oscillatory steady state is discovered in observation of potential with a heavy ion beam probe in Compact Helical System heliotron/torsatron. Bulk plasma parameters, such as electron temperature and density profile, change synchronously with the pulsation of potential. The phenomenon can be regarded as successive transitions between two bifurcative states of the plasma. The pulsation can be self-sustained and create a dynamic steady state in low density plasmas with electron cyclotron heating. The cause of the phenomenon is associated with the bifurcation nature of radial electric field, that is inherent in toroidal helical plasmas. This paper presents two examples of the phenomenon in different density regimes. Dependence of pulsation characteristics on several parameters is described. The bifurcation property predicted by a neoclassical theory is presented for comparison with the experimental observations.

TH2/1: 5D simulation study of suprathermal electron transport in nonaxisymmetric plasmas

M. Murakami et al.

ECRH-driven transport of suprathermal electrons is studied in nonaxisymmetric plasmas using a new Monte Carlo simulation technique in 5D phase space. Two different phases of the ECRH-driven transport of suprathermal electrons can be seen; one is a rapid convective phase due to the direct radial motion of trapped electrons and the other is a slower phase due to the collisional transport. The important role of the radial transport of suprathermal electrons in the broadening of the ECRH deposition profile is clarified in W7-AS. The ECRH-driven flux is also evaluated and put in relation with the "electron root" feature recently observed in W7-AS. It is found that, at low collisionalities, the ECRH-driven flux due to the suprathermal electrons can play a dominant role in the condition of ambipolarity and, thus, the observed "electron root" feature in W7-AS is thought to be driven by the radial (convective) flux of ECRH-generated suprathermal electrons. The possible scenario of this "ECRH-driven electron root" is considered in the LHD plasma.

FT1/3(R): LHD-Type compact helical reactors

A. Sagara et al.

From the point of view of D-T fusion demonstration reactors, the LHD-type helical reactor designs are studied to clarify design issues for realizing compact reactors, where the major radius R should be as small as possible. The LHD concept is characterized by two advantages: (1) simplified superconducting continuous-coil system and (2) efficient closed helical divertor. Therefore, on the basis of physics and engineering results established in the LHD project, which has already started plasma confinement experiments, two possible approaches on to reactor designs are investigated: increasing the toroidal field B_0 in the concept of Force-Free Helical Reactor (FFHR) with a continuous-coil system, and increasing the plasma minor radius a_p in the concept of Modular Heliotron Reactor (MHR) with an efficient closed divertor. Physics and engineering results are presented, including new proposals.

FT2/1: Progress summary of LHD engineering design and construction

O. Motojima et al.

In March 1998, the Large Helical Device (LHD) project finally completed its 8-year construction schedule. LHD is a superconducting (SC) heliotron type device with R = 3.9 m, a_p = 0.6 m, and B = 3 T, which has simple and continuous large helical coils. The major mission of LHD is to demonstrate the high potential of currentless helical-toroidal plasmas, which are free from current disruption and have an intrinsic potential for steady-state operation. After the intensive physics design studies in the 1980s, the necessary programs of SC engineering R&D were made and carried out, and as a result, LHD fabrication technologies were successfully developed. In this process, a significant data base on fusion engineering has been established. These achievements have been made in various areas, such as the technologies of SC conductor development, SC coil fabrication, liquid helium (LHe) and supercritical helium (SHe) cryogenics, development of low temperature structural materials and welding, operation and control, and power supply systems and related SC coil protection schemes. They are integrated and nowadays comprise a major part of the LHD relevant fusion technology area. These issues correspond to a necessary technological data base for the next step of future reactor designs. In addition, we could increase this with successful commissioning tests just after the completion of LHD machine assembly phase, which consisted of vacuum leak test, LHe cooldown test, and coil current excitation test. We recapitulate and highlight these LHD relevant engineering developments in this paper. To summarize our construction of LHD as an SC device, the critical design with NbTi SC material has been successfully accomplished by our R&D activities, which enables us to move into a new regime of fusion experiments.

EXP1/18: Particle transport study with tracer-encapsulated solid pellet injection

S. Sudo et al.

In order to promote particle transport studies, a tracer-encapsulated solid pellet (TESPEL) is proposed to observe the behavior of tracer particles deposited locally. TESPEL consists of polystyrene as an outer part and LiH as an inner core. For proving the essential concept of the new diagnostics, TESPEL is injected into a neutral-beam-heated

plasma of the Compact Helical System. This experiment shows the successful local deposition of the tracer, and the behavior of tracer particles deposited locally in the plasma core region is also observed by a method of charge exchange recombination spectroscopy. Thus, our new diagnostic concept has been proven for the first time from the viewpoints of both the production method of a tracer-encapsulated pellet as well as from the observation of the tracer particles.

EXP1/19: Global MHD modes excited by energetic ions in heliotron/torsatron plasmas

K. Toi et al.

In NBI heated plasmas of the CHS heliotron/torsatron where the beam driven current with a peaked profile is induced, $m = 2/n = 1$ and $m = 3/n = 2$ (m, n: poloidal and toroidal mode numbers) fishbone instabilities are observed for the first time. Pulsed increase in energetic ion loss flux is detected by an escaping ion probe during the $m = 3/n = 2$ mode. The sawtooth crash is often induced by the $m = 2/n = 1$. The current-driven internal kink mode is thought to be destabilized by the presence of energetic ions, having a character of pressure driven interchange mode. Toroidal Alfvén eigenmodes (TAEs) with $n = 1$ and $n = 2$ are also identified for the first time in NBI heated plasmas. TAEs localize near the plasma core region with fairly low magnetic shear realized by the small net plasma current, and do not lead to enhanced loss of energetic ions because of low fluctuation levels.

THP1/8: Global mode analysis of ideal MHD modes in $\ell = 2$ heliotron/torsatron systems

N. Nakajima et al.

By means of a global mode analysis of ideal MHD modes for Mercier-unstable equilibria in a planar axis $\ell = 2/M = 10$ heliotron/torsatron system with an inherently large Shafranov shift, the conjecture from local mode analysis for Mercier-unstable equilibria has been confirmed and the properties of pressure-driven modes have been clarified. According to the degree of the decrease in the local magnetic shear by the Shafranov shift, the Mercier-unstable equilibria are categorized into toroidicity-dominant (strong reduction) and helicity-dominant (weak reduction) equilibria. In both types of equilibria, interchange modes are destabilized for low toroidal mode numbers $n < M$, where M is the toroidal field period of the equilibria, and both poloidally and toroidally localized ballooning modes purely inherent to three-dimensional systems are destabilized for fairly high toroidal mode numbers $n > M$. For moderate toroidal mode numbers $n \sim M$, tokamak-like poloidally localized ballooning modes with a weak toroidal mode coupling are destabilized in toroidicity-dominant equilibria; in contrast, in the helicity-dominant equilibria, interchange modes are destabilized. The interchange modes are localized on the inner side of the torus, because the Shafranov shift enhances the unfavorable magnetic curvature there rather than on the outer side of the torus. A continuous or quasipoint unstable spectrum is briefly discussed.

FTP/21: Steady-state heating technology development for LHD

T. Watari et al.

Construction of the LHD has been completed and the experimental phase began in early April 1998. The first plasma was obtained with ECH with a power level of 300 kW. Three heating schemes, ECH, ICRF, and NBI, are adopted and join the heating experiment in the second experimental campaign. Since the LHD has superconducting coils, one of the missions of plasma heating in the LHD is demonstration of a steady-state plasma. Intensive technology development for steady-state plasma heating has been carried out at NIFS since 1992. The paper summarizes the achievements of these developmental activities in the past several years. The knowledge obtained may be applicable to ITER, where steady-state plasma heating is essential.

FTP/02(R): Coil system of a Helias reactor

J. Kisslinger, C. D. Beidler, E. Harmeyer, F. Herrnegger, H. Wobig, and W. Maurer

The magnetic fields of advanced stellarator configurations can be generated by 3D shaped modular coils. The shapes of these coils are calculated for a given Helias field configuration. This method allows one to optimize the field according to criteria of optimum plasma performance in a preceding step. The coil system of the Helias reactor considered here is roughly four times as large as that of the Wendelstein 7-X device and produces about the same field configuration. The maximum field strength of 10 T at the coils is small enough to use NbTi superconductors at 1.8 K. The "cable-in-conduit" conductor is designed for a nominal current of 37.5 kA and has an aluminum alloy jacket. In order to reduce the maximum field on the conductor, the winding pack of each coil is split into two rectangular parts with 9×16 turns each. These two subwinding packs are in a common enclosing coil housing with a central web for mechanical stiffening. The coils are mutually connected by support elements forming a toroidal vault. Finite-element calculations show that the coils tend to become more circular and planar under the magnetic force load and require local reinforcements of the coil housings.

CDP/05: ECRH and ECCD experiments in an extended power range at the W7-AS stellarator

V. Erckmann, U. Gasparino, H. P. Laqua, H. Maaßberg, W7-AS Team, K.S. Kasilov, N. Marushchenko, V. Irkhin, and S. Malygin

An overview of physics studies on electron cyclotron resonance heating (ECRH) and EC current drive (ECCD) in an

extended parameter range at W7-AS is presented. Experiments were performed with an upgraded ECRH power of up to 1.3 MW at 140 GHz. Electron temperatures of up to 5.7 keV were measured, which can only be explained by the beneficial effect of positive radial electric fields ("electron root"). The experiments confirm, that the electric field is generated by ECRH-driven particle losses in the specific stellarator magnetic field. ECCD experiments were performed at high input power (1.3 MW) resulting in EC-driven currents of up to 20 kA. The direction of the EC-driven current was varied in co- and counter-direction with respect to the bootstrap current in discharges with zero net current. Three current contributions, i.e. the EC-driven current, the bootstrap current, and the inductively driven current are calculated independently and modify the internal profile of the rotational transform significantly. A comparison with quasilinear theory shows significant deviation in the co-current drive case, which may be attributed to strong MHD activity and/or violation of the quasilinear assumptions due to the high power density.

CD1/5: Plasma heating and sustainment in the ion cyclotron range of frequencies on the stellarator W7-AS

Dirk A. Hartmann, G. Cattanei, ICRH Group, W7-AS Team

On the stellarator W7-AS resonant and nonresonant ICRF heating scenarios were successful both in increasing the ion and electron temperature of ECRH or NBI target plasmas and in sustaining the plasmas under steady-state conditions. The investigated scenarios were: D(H), ^{4}He(H) minority heating (minority species in brackets), D/H mode conversion heating and second harmonic H heating. In all cases density control was possible and no significant increase in impurities was observed. The heating efficiencies were comparable to tokamaks.

THP1/05: Dimensionless energy confinement scaling in W7-AS

R. Preuss, V. Dose, and W. von der Linden

Energy confinement in W7-AS has been analyzed in terms of dimensionally exact form-free functions employing Bayesian probability theory. The confinement function was set up as a linear combination of dimensionally exact power law terms as already proposed very early by Connor and Taylor. Generation of this expansion basis is dictated by the basic plasma model which one assumes. Based upon data accumulated in W7-AS, which contains the stored energy for a wide variety of variable settings, predictions for single variable scans are made. The scaling functions for density and power scans, respectively, are in quantitative agreement with data collected in W7-AS. The result of a single variable scan is therefore already hidden in the data obtained for arbitrary variable choices and can be extracted from the latter by a proper data analysis. Furthermore, the optimal model for the description of the global transport in W7-AS is identified as the collisional low beta kinetic model.

OV2/4: Overview on W7-AS results with relevance for Wendelstein 7-X and the low-shear stellarator line

F. Wagner et al.

The Wendelstein stellarator program of Garching has developed low-shear stellarators with successively optimized designs to remove the intrinsic deficiencies of this 3D concept. W7-X, presently under construction, is in internal terminology a fully optimized stellarator. W7-AS, the presently operated device, is a partly optimized stellarator. The optimization of stellarators aims at improved neoclassical confinement in the long mean-free-path regime and improved equilibrium and stability properties. In this report, we address equilibrium, stability, turbulent and collisional energy confinement aspects (role of shear, role of the radial electric field, low and improved confinement regimes), particle transport, edge transport and turbulence, high density operation, ECRH (OXB scheme) and ICRF heating and the development of the island divertor for exhaust. The maximal parameters achieved in W7-AS (at different discharge types) are: T_e = 5.8 keV, T_i = 1.5 keV, $n_e = 3 \times 10^{20}$ m^{-3}, $\langle\beta\rangle$ = 2%, τ_E = 50 ms.

EX2/1: Investigation of equilibrium, global modes and microinstabilities in the stellarator W7-AS

A. Weller et al.

Equilibrium and stability properties in the Wendelstein 7-AS stellarator are investigated experimentally and compared with theoretical predictions for particular cases. The topology of equilibrium magnetic surfaces and of global MHD modes is inferred from X-ray tomography. The predicted effects of externally driven currents and internal currents on the equilibrium surfaces could be confirmed experimentally. In particular the reduced Shafranov shift due to reduced Pfirsch-Schlüter currents in W7-AS could be verified. Up to the maximum accessible beta ($\beta \sim 1.9\%$) plasmas can be confined without significant deterioration by pressure driven MHD activity. However, global modes in the stable MHD spectrum such as global and toroidal Alfvén eigenmodes (GAE, TAE) can be destabilized by energetic ions from neutral beam heating. These instabilities appear as very coherent low frequency modes (= 40 kHz) in the lower β regime without significant impact on the global confinement. At medium β very strong particle driven MHD with frequencies up to the range of 500 kHz can be observed. These modes can show nonlinear behavior including periodic bursting and frequency chirping in combination with significant plasma energy losses. With increasing β Alfvén modes are widely stable, because under these conditions the damping relative

to the particle drive is increased. Besides the global mode activity, small-scale turbulent structures have been investigated in the plasma core and at the edge. The measured data of electron temperature, density and magnetic fluctuations do not yet allow to assess turbulence driven transport fluxes. However, correlations with the global confinement have been found, and the measured amplitudes are in the range expected to be relevant for anomalous transport. The observed dependence of the confinement on the edge rotational transform and magnetic shear can be explained in terms of enhanced transport at rational surfaces; however, the underlying mechanism is still unclear.

ICP/07: Design studies of low-aspect ratio quasiomnigenous stellarators

D. A Spong, S. P. Hirshman, J. C. Whitson, et al.

Attractive 3- and 4-field period low aspect ratio quasiomnigenous (QO) stellarators have been designed based on a set of optimization criteria chosen to lead to a compact reactor. Transport and energetic particle confinement are improved over conventional stellarators by targeting alignment of the longitudinal adiabatic invariant and magnetic flux contours (quasiomnigeneity). Stability is targeted by requiring the presence of a magnetic well and favorable Mercier stability. Realizable coil geometries are achieved by targeting low ripple and considering only low field period devices (2–4). Low (but finite) bootstrap current is maintained while creating most (> 70%) of the rotational transform through plasma surface shaping. This process has resulted in a range of designs which lead both to interesting near-term concept exploration devices (B_0 = 1 T, R_0 = 1 m) as well as good extrapolation to reactor configurations.